

Corrosion of Fresh Porous Silicon in Potassium Hydroxide Solution

Zhen Xiang^{1,*}, Changlu Liu², Chuan Lai²

¹ School of Chemistry and Pharmaceutical Engineering, Sichuan University of Science & Engineering, Zigong 643000, PR China

² School of Chemistry and Chemical Engineering, Sichuan University of Arts and Science, Dazhou 635000, PR China

*E-mail: tougaolc@126.com

Received: 6 November 2014 / Accepted: 18 February 2015 / Published: 23 March 2015

Porous silicon samples were fabricated by electrochemical anodization of silicon wafers. After fabricating, the corrosion of fresh porous silicon (f-PS) in potassium hydroxide solution in the absence and presence of ethanol was systemically studied by electrochemical methods, weight loss measurements and scanning electron microscope. The effect factors for f-PS corrosion in KOH solution were investigated. It found that the temperature and composition of corrosion solution can affect the detection accuracy of weight loss measurements to measure the porosity of f-PS. In addition, the activation parameters (E_a , A , ΔH_a and ΔS_a) for f-PS in 1.0 M KOH were obtained.

Keywords: Polarization; SEM; Weight loss; Alkaline corrosion.

1. INTRODUCTION

Porous silicon (PS) was accidentally discovered in 1956 by Uhlir when he was trying to develop an electrochemical method to machine silicon wafers [1-2]. However, the more interest in PS was developed after the demonstration of efficient visible photoluminescence from the PS by Canham in early 1990 [3]. With this discovery, the PS has attracted increasing interest for various potential applications including electronics, photonics and biosensing [4-7], such as an insulating layer in the silicon-on-insulator [8-9], a sensing layer in biosensors [9] or chemical sensors [10], an energy carrier [11], a sacrificial layer in micromachining [12], as an important material for solar cell [13] and many others [14-16]. However, there are few works focusing on the applications of PS in alkaline solution resulting from the corrosion and dissolution of PS in it [17-21].

In order to measure the porosity of PS by weight loss measurements, the different concentration of sodium hydroxide (NaOH) or potassium hydroxide (KOH) solution were used to remove PS layer [9, 17, 20, 22]. Based on previous works [9,17, 20, 22], although the PS layer can dissolve in the aqueous solution of NaOH or KOH, but there are few studies focusing on the corrosion and dissolution of PS in alkaline solution, especially the detection accuracy of weight loss measurements to measure the porosity of PS.

As a result, the main objective of the present work was to investigate the corrosion of f-PS in alkaline solution. At the beginning, several f-PS samples were fabricated by electrochemical anodization. Then their corrosion behavior in KOH solution in the absence and presence of ethanol was systemically studied using electrochemical methods, weight loss measurements and scanning electron microscope.

2. EXPERIMENTAL

2.1 Reagents and materials

Hydrofluoric acid (HF, 40%, A. R.), ethanol (EtOH, 99.5%, A. R.), acetone (A. R.), potassium hydroxide (KOH, A. R.), were purchased from Sinopharm Chemical Reagent Co., Ltd. All the reagents were commercially available and used without further purification. Silicon wafers, a phosphorus doped n-type wafer with a resistivity of 2-4 Ω cm, (100) oriented and 500-550 μ m thick, was purchased from Emei Semiconductor Material Institute (China). Double distilled water was used in the experiments. The etching solution (1:1 (v/v) EtOH(99.5%)/HF(40%)) and corrosion solution (the aqueous solution of KOH in the absence and presence of ethanol.) were used to prepare porous silicon (PS) and remove PS layer, respectively.

2.2 Fabrication of porous silicon samples

Porous silicon samples, composed of PS layer with the same total surface areas of 0.95 cm² and silicon substrate, were fabricated by electrochemical anodization of silicon wafers in a solution of 1:1 (v/v) EtOH(99.5%)/HF(40%) [7]. The electrochemical process was performed in a Teflon cell using two-electrode configuration with a Pt gauze as the cathode and silicon substrate as the anode, under the illuminating of 150 W high pressure mercury lamp and at a constant current density of 30 mA cm⁻² for 30 min. After fabrication, the fresh porous silicon (f-PS) were rinsed with ethanol and acetone and then stored in ethanol to prevent oxidization.

2.3 Electrochemical measurements

Electrochemical measurements were carried out using a conventional three-electrode cell consisting of a f-PS working electrode (0.95 cm²), a platinum gauze counter electrode and a silver-silver chloride (Ag/AgCl) electrode as a reference electrode. Potentiodynamic (Tafel) polarization and

linear polarization measurements were carried out by a computer controlled CHI 660b Electrochemical Workstation (Shanghai, China) to investigate the electrochemical behavior of f-PS corrosion in KOH solution in the absence and presence of ethanol.

As to linear polarization measurements, the potential of the electrode was scanned from -20 mV to 20 mV vs. corrosion potential at scan rate of 0.166 mV s^{-1} and the polarization resistance was calculated from the slope of potential vs. current curve in the vicinity of corrosion potential. Tafel polarization curves were obtained in the potential range of -350 mV to +350 mV in regard to open circuit potential. The corrosion current densities were estimated by extrapolation of the anodic and cathodic Tafel lines.

In this paper, it should be noted that the electrochemical corrosion behavior of f-PS in KOH solution was investigated at a relative low temperature of 291 K due to the existence of plenty of bubbles formation from the f-PS layer in KOH solution at the higher temperature (above 298 K), which would affect the accuracy of electrochemical measurements.

2.4 Weight loss measurements

Weight loss measurements were carried out in 250 mL beaker, which contained 100 mL corrosion solution, at different temperature controlled by a water thermostat. All the test solutions were open to air. The mass of cleaned and dried porous silicon samples before and after corrosion in the test solutions was determined using an analytical balance of 0.01 mg accuracy. After weighted, three parallel porous silicon samples were immersed in a beaker with test solutions for different time, where the time is defined as immersion time. Then the immersed samples were rinsed thoroughly with double distilled water, ethanol and acetone successively. After rinsed, the samples were dried and re-weighed accurately. Triplicate experiments were performed in each case and the mean value of the weight loss was calculated. The corrosion rate was obtained according to Eq. (1) [23-24]:

$$v = \frac{m_{f1} - m_{f2}}{St} = \frac{\Delta m_f}{St} \quad (1)$$

where m_{f1} is the mass of the f-PS before corrosion, m_{f2} is the mass of the f-PS after corrosion, Δm_f is the mass change of f-PS before and after corrosion for different time, S is the total area of the f-PS (0.95 cm^2), t is the immersion time and v is the corrosion rate.

In the present work, it need to be mentioned that the corrosion time was defined as the time when PS layer was completely removed from PS sample in corrosion solution, and it mainly depended on the thickness of porous layer, temperature and the composition of KOH solution.

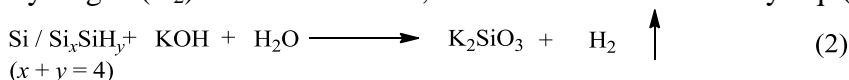
2.5 Scanning electron microscope

The microstructures of f-PS samples before and after corrosion in 1.0 M KOH solution for different immersion time were analyzed by scanning electron microscope (SEM, TESCAN VEGA 3 and FEI Nova400).

3. RESULTS AND DISCUSSION

3.1 Corrosion process

It is well known that there are various kinds of activated Si—H bonds on the PS layer (Si_xSiH_y ($x+y=4$)) [25-27]. Both PS layer and silicon substrate (Si) can react with the aqueous solution of KOH to form hydrogen (H_2) and dissolve in it, which can be illustrated by Eq. (2) [28-29]:



At the beginning of f-PS samples corrosion and dissolution in KOH solution, there were plenty of bubbles generated from the f-PS layer and the color of f-PS changed from khaki to light yellow, then to dark grey. As the corrosion and dissolution of PS layer continued, the color changed from dark grey to black. Along with the corrosion reaction, the black PS layer turned into a black patch, and then changed into a black spot. Finally, the f-PS layer was completely removed by the KOH solution. A set of changes in the color of f-PS reflected the degree of the porosity, thickness and oxidation of f-PS in KOH solution.

3.2 Electrochemical behavior

3.2.1 Linear polarization measurements

Fig. 1 revealed the typical linear polarization curves for f-PS in 1.0 M KOH in the absence and presence of 30% ethanol (1.0 M KOH-30%EtOH) at 291 K. Meanwhile, the linear polarization resistances (R_p , Ohms cm^{-2}) for f-PS in different concentration of KOH and 1.0 M KOH with different volume ratio of ethanol was shown in Fig. 2a and b, respectively.

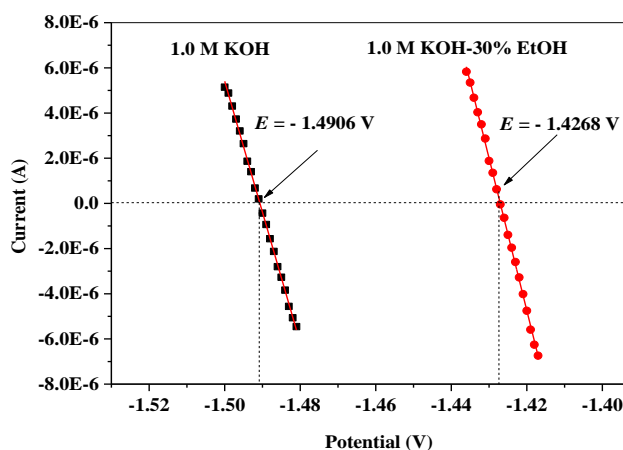


Figure 1. The typical experimental linear polarization curves for f-PS in 1.0 M KOH in the absence and presence of 30% ethanol at 291 K.

Fig. 2a illustrated the effect of KOH concentration on the R_p at 291 K. The value of R_p obtained from linear polarization measurements decreased from 3634.1 to 1679.1 Ohms cm^{-2} in the range of 0.1 to 2 M, which indicated that the corrosion rate increased with concentration of KOH increasing.

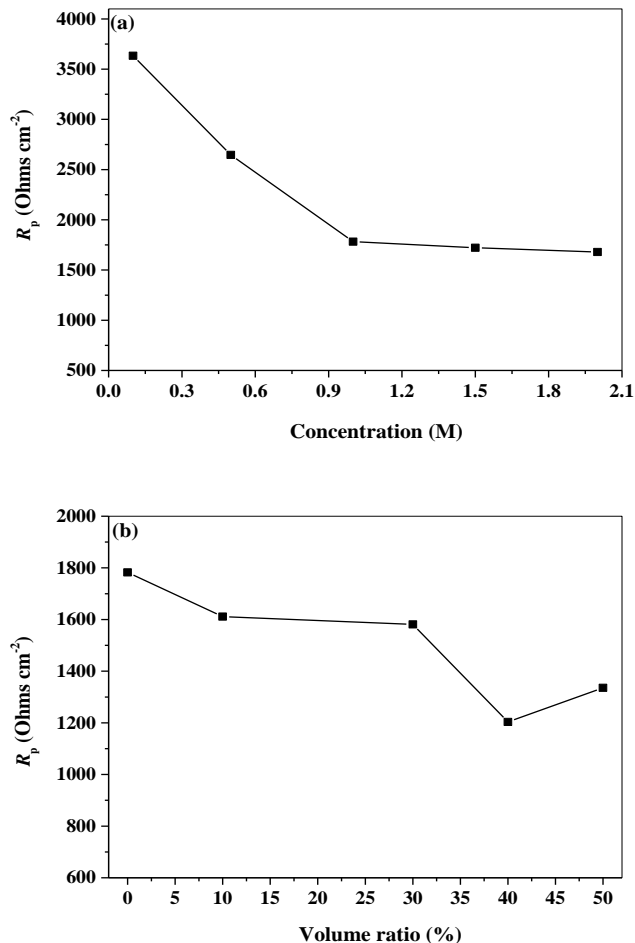


Figure 2. The effects of concentration and volume ratio of ethanol on linear polarization resistance for f-PS in KOH solution at 291 K.

Fig. 2b showed typical relationship between the R_p and the volume ratio of ethanol in 1.0 M KOH at 291 K. The value of R_p decreased with the volume ratio of ethanol increasing until reached the minimum value (1203.5 Ohms cm^{-2} , where the volume ratio of ethanol is 40%) and then increased slightly when volume ratio increases to 50%. The result was well consistent with the fact that solvent H_2O directly participated in the corrosion reaction as shown in Eq. (2) and the numbers of H_2O molecules decreased with the increase of ethanol volume ratio in 1.0 M KOH. The obvious decrease of R_p indicated that the addition of ethanol in KOH solution can increase the corrosion rate, possibly because ethanol can reduce the surface tension of alkaline solution and increase wettability of PS surface [30-31].

3.2.2 Potentiodynamic polarization measurements

Polarization behaviors for f-PS in KOH solution in the absence and presence of ethanol were shown in Fig. 3a and b. The values of corrosion potential (E_{corr}), cathodic and anodic Tafel slopes b_c and b_a (V dec^{-1}) and corrosion current density (I_{corr}) as functions of KOH concentration and volume ratio of ethanol in 1.0 M KOH, were calculated from the curves in Fig. 3 and listed in Table 1.

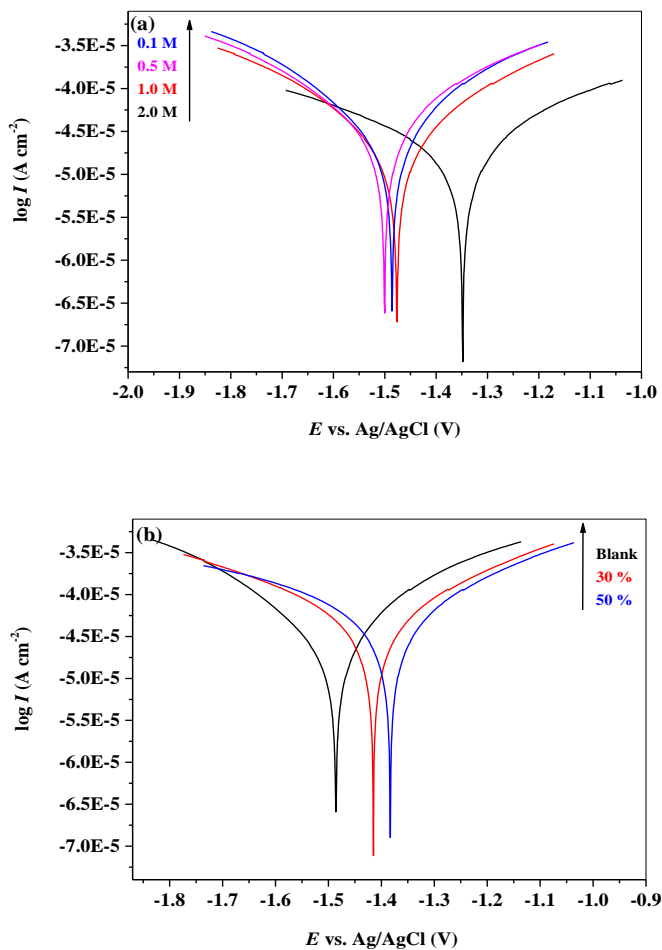


Figure 3. Potentiodynamic polarization curves for f-PS in KOH solution in the absence and presence of ethanol at 291 K, (a) different concentration of KOH, (b) different volume ratio of ethanol in 1.0 M KOH.

At 291 K, the E_{corr} shifted significantly to more negative potentials and the I_{corr} increased with concentration of KOH increasing (Fig. 3a and Table 1). It indicated that KOH with high concentration can cause serious corrosion of the f-PS [32-33].

Fig. 3b showed that the addition of ethanol in 1.0 M KOH shifted the E_{corr} values towards the positive (-1.383 V and -1.415 V in the presence of 30% and 50% ethanol compared with that measured in blank solution -1.486 V). The significant increase in the value of I_{corr} for f-PS corrosion also indicated that the addition of ethanol in KOH solution can increase the corrosion rate [33]. There was a good agreement between potentiodynamic polarization and linear polarization measurements, where

the two different techniques gave the same trend of f-PS corrosion in different concentration of KOH solution in the absence and presence of ethanol.

Table 1. Potentiodynamic polarization parameters for f-PS in KOH solution in the absence and presence of ethanol at 291 K.

Corrosion solution	E_{corr} vs. Ag/AgCl (V)	I_{corr} (A cm^{-2}) $\times 10^{-5}$	b_a (V dec^{-1})	b_c (V dec^{-1})
0.1 M KOH	-1.348	1.264	0.2287	0.1774
0.5 M KOH	-1.476	1.585	0.1820	0.1648
1.0 M KOH	-1.486	2.127	0.1868	0.1554
2.0 M KOH	-1.500	2.647	0.2086	0.1731
1.0 M KOH/30%EtOH	-1.415	3.205	0.2073	0.1866
1.0 M KOH/50%EtOH	-1.383	3.222	0.2146	0.1841

3.3 Weight loss measurements

3.3.1 Corrosion rate

The relationship between mass change ($\Delta m_f/S$) and immersion time (t) for f-PS in 1.0 M KOH at different temperatures was shown in Fig. 4. According to Eq. (1) and Fig. 4, the corrosion rate was determined by linear regression between mass change ($\Delta m_f/S$) and immersion time, and all curves showed a good linear relationship ($R > 0.98$). Based on the slopes of curves, the corrosion rate for f-PS corrosion in 1.0 M KOH could be obtained. When temperatures were 303, 313 and 333 K, the corrosion rates were 114.00, 322.44 and 674.22 $\text{g m}^{-2} \text{h}^{-1}$, respectively.

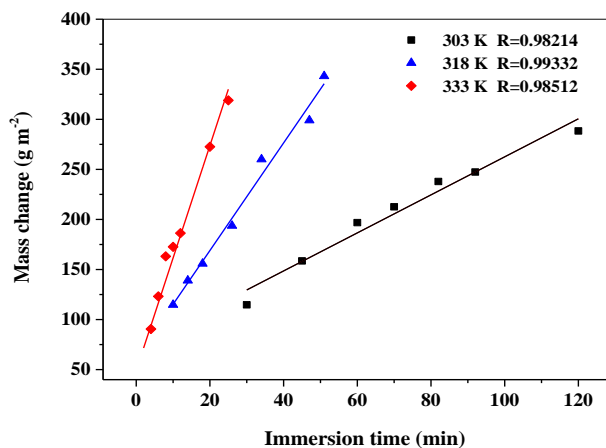


Figure 4. The relationships between mass change and immersion time for f-PS in 1.0 M KOH at different temperatures.

3.3.2 Effect factors

Fig. 5 reported the effect of KOH concentration on corrosion rate and corrosion time at 318 K. As seen from Fig. 5, the corrosion rate increased and the corrosion time decreased as the concentration of KOH increased. The corrosion rate elevated from 174.71 to 348.27 $\text{g m}^{-2} \text{h}^{-1}$ when the concentration of KOH increased from 0.05 to 2.0 M. This result indicated that the high concentration of KOH could increase the corrosion rate. Furthermore, as the concentration changed from 0.05 to 1.0 M, the corrosion time varied from 130 to 58 min. When the concentration of KOH was higher than 1.0 M, the corrosion time seldom changed. So we chose the 1.0 M KOH solution to investigate other effect factors.

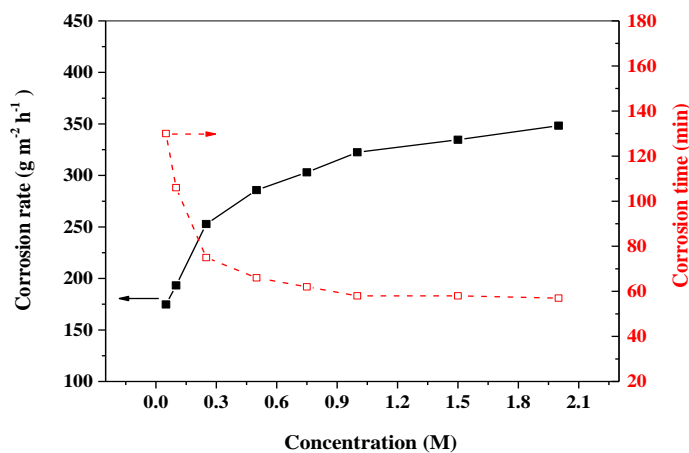


Figure 5. The corrosion rate and corrosion time for f-PS in different concentration of KOH solution at 318 K.

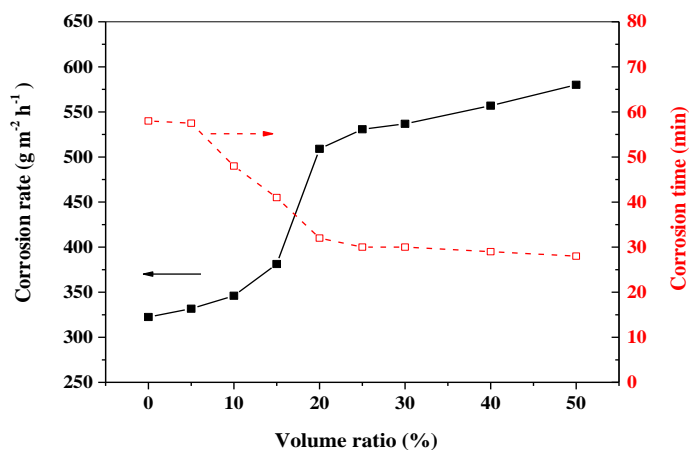


Figure 6. The corrosion rate and corrosion time for f-PS in 1.0 M KOH with different volume ratio of ethanol at 318 K.

Fig. 6 revealed that the corrosion rate and corrosion time were remarkably affected by the volume ratio of ethanol in 1.0 M KOH at 318 K. The corrosion rate went up with the increasing

volume ratio of ethanol in 1.0 M KOH. The reason of the different tendency between weight loss measurements and electrochemical measurements was that the measurements were conducted at the different temperature. Obviously, adding ethanol into KOH solution can dramatically improve corrosion rate and shorten the corrosion time. It can be easily achieved that the corrosion time decreased with the increasing volume ratio of ethanol. In this experiment, the 1.0 M KOH containing 30% ethanol was chose as the corrosion media to study other effect factors.

The effect of temperature for f-PS corrosion in 1.0 M KOH in the absence and presence of 30% ethanol (1.0 M KOH-30%EtOH) was shown in Fig. 7. It was apparent that with the temperature increasing, the corrosion rate and corrosion time clearly increased and decreased, respectively. The result was reasonable and consistent with the results reported by Ebenso [34] and Chuan [35]. At the same temperature, the corrosion rate in 1.0 M KOH (113.68-675.79 g m⁻² h⁻¹) was lower than that in 1.0 M KOH containing 30% ethanol (271.58-727.69 g m⁻² h⁻¹), and the corrosion time in 1.0 M KOH (130-25 min) was longer than that in 1.0 M KOH with 30% ethanol (60-23 min). The shorter of the corrosion time is, the faster of the corrosion rate will be. The studies for variation tendency for f-PS corrosion process by weight loss measurements were correspond to that by electrochemical measurements.

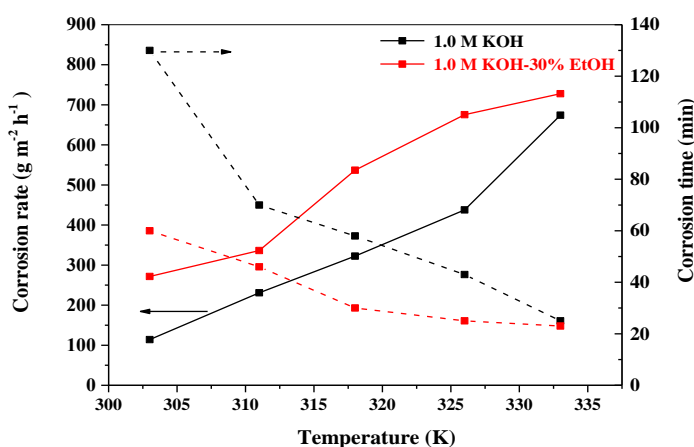


Figure 7. The corrosion rate and corrosion time for f-PS in 1.0 M KOH in the absence and presence of 30% ethanol at different temperatures.

3.4 Detection accuracy of mass change

Porosity (*P*) is the key properties of PS, which can usually be estimated by weight loss measurements according to Eq. (3) and (4) [19, 21, 25, 36]:

$$P (\%) = \frac{m_1 - m_2}{m_1 - m_3} \times 100 \tag{3}$$

$$m_1 - m_3 = (m_1 - m_2) + (m_2 - m_3) = (m_1 - m_2) + \Delta m \tag{4}$$

where *m*₁ is the mass of the sample before PS formation, *m*₂ is the mass after formation, *m*₃ is the mass of the PS sample after PS layer completely removed by corrosion solution.

Table 2. The mass change of f-PS completely removed by different composition of KOH solution at different temperatures.

Corrosion solution	Temperature (K)	Mass change (g)
1.0 M KOH	303	0.0358
1.0 M KOH	318	0.0380
1.0 M KOH	333	0.0387
1.0 M KOH-30%EtOH	318	0.0348

The mass change (m_1-m_2) under the identical conditions of fabrication should be a constant value. Based on Eq. (4), the precision value of PS layer mass, defined by the mass change (Δm), determine the accuracy of detection of porosity. Usually, the KOH solution with different concentration could be used to remove PS layer for measuring porosity. However, there was no standard to choose the corrosion solution and no studies focus on the effect of different composition of corrosion solution for removing PS layer on the detection accuracy of weight loss measurements to measure the porosity. In this work, the mass change (Δm) was obtained from using different composition of KOH solution to remove f-PS layer which was listed in Table 2. From Table 2, Eq. (3) and (4), it was apparent that the temperature and composition of KOH solution could affect the accuracy of mass change (Δm), thus affecting the detection accuracy of weight loss measurements for measuring the porosity. This is due to both PS layer and silicon substrate can dissolve in KOH solution.

3.5 Activation parameters

Arrhenius Eq. (5) and transition state Eq. (6) [37-40] were used to calculate activation parameters (E_a , A , ΔH_a and ΔS_a) for f-PS corrosion in 1.0 M KOH in the absence and presence of 30% ethanol (1.0 M KOH-30%EtOH).

$$\ln v = \ln A - \frac{\Delta E_a}{RT} \quad (5)$$

$$\ln \frac{v}{T} = \left(\ln \frac{R}{Nh} + \frac{\Delta S_a}{R} \right) - \frac{\Delta H_a}{RT} \quad (6)$$

where v is the corrosion rate, A is the Arrhenius pre-exponential factor, E_a is the activation energy, h is the Planck's constant, N is the Avogadro's number, R is the universal gas constant, T is the absolute temperature, ΔH_a is the enthalpy of activation and ΔS_a is the entropy of activation.

According to Eq. (5) and (6), Arrhenius plots of $\ln v$ vs. $1000/T$ and $\ln(v/T)$ vs. $1000/T$ for f-PS in 1.0 M KOH with and without 30% ethanol were shown in Fig. 8a and b. The calculated values of activation energy (E_a), Arrhenius pre-exponential factor (A), enthalpy of activation (ΔH_a) and entropy of activation (ΔS_a) were listed in Table 3.

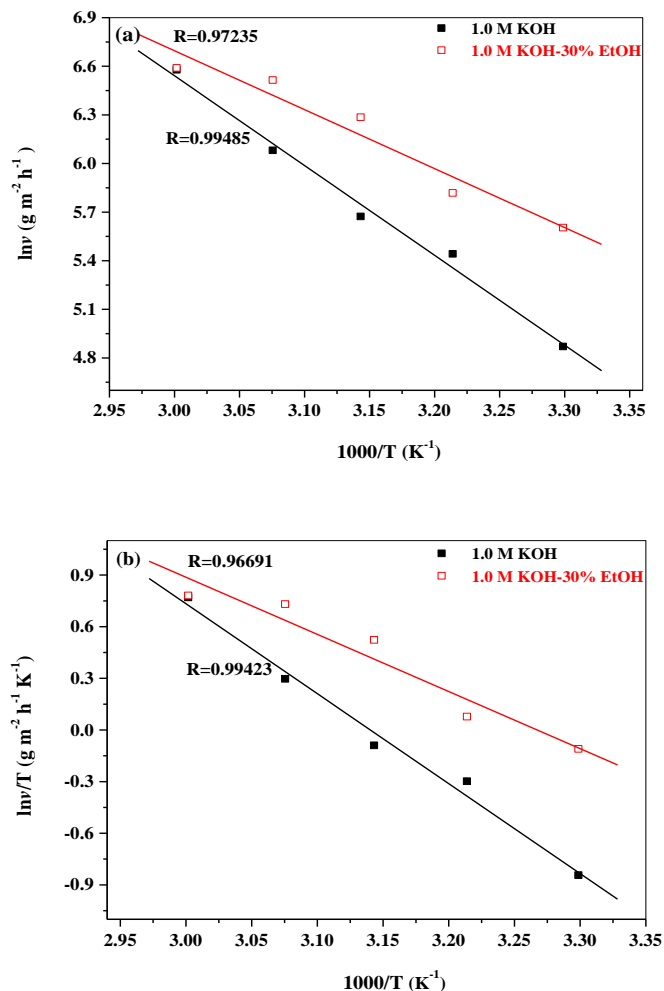


Figure 8. Arrhenius plots of $\ln v$ vs. $1000/T$ and $\ln(v/T)$ vs. $1000/T$ for f-PS corrosion in 1.0 M KOH in the absence and presence of 30% ethanol.

As can be seen from Fig. 8a, the good linear relationship between $\ln v$ and $1000/T$ ($R > 0.97$), indicated that the corrosion of f-PS in 1.0 M KOH with and without 30% ethanol could be elucidated by Arrhenius kinetic model. The activation energy for f-PS in 1.0 M KOH ($46.06 \text{ kJ mol}^{-1}$) was higher than that in 1.0 M KOH containing 30% ethanol ($30.25 \text{ kJ mol}^{-1}$). This showed that in the presence of ethanol as additive, the energy barrier of the corrosion reaction would relatively decrease. According to Eq. (5), it can be concluded that the higher Arrhenius pre-exponential factor and the lower activation energy lead to the higher corrosion rate. In this work, the Arrhenius pre-exponential factor and activation energy in 1.0 M KOH were higher than that in 1.0 M KOH with 30% ethanol, respectively. Therefore, the increase of corrosion rate was determined by the apparent activation energy. The decrease of activation energy also demonstrated that ethanol can decrease surface tension of KOH solution and improve the corrosion rate [33].

Table 3. The activation parameters for f-PS corrosion in 1.0 M KOH in the absence and presence of 30% ethanol.

Corrosion solution	E_a (kJ mol ⁻¹)	A (g m ⁻² h ⁻¹)	ΔH_a (kJ mol ⁻¹)	ΔS_a (J K ⁻¹ mol ⁻¹)
1.0 M KOH	46.06	1.160×10^{10}	43.40	-61.11
1.0 M KOH-30%EtOH	30.25	4.450×10^7	27.61	-107.33

Fig. 8b revealed the relationship between $\ln(v/T)$ and $1000/T$. Straight lines were obtained with a slope of $-\Delta H_a/R$ and an intercept of $\ln(R/Nh) + \Delta S_a/R$ from which the enthalpy of activation and entropy of activation were calculated and listed in Table 3. The enthalpy of activation of f-PS in 1.0 M KOH (43.40 kJ mol⁻¹) was higher than that in 1.0 M KOH containing 30% ethanol (27.61 kJ mol⁻¹). The entropy of activation in 1.0 M KOH (-61.11 J K⁻¹ mol⁻¹) was higher than that in 1.0 M KOH with 30% ethanol (-107.33 J K⁻¹ mol⁻¹).

3.6 Scanning electron microscope

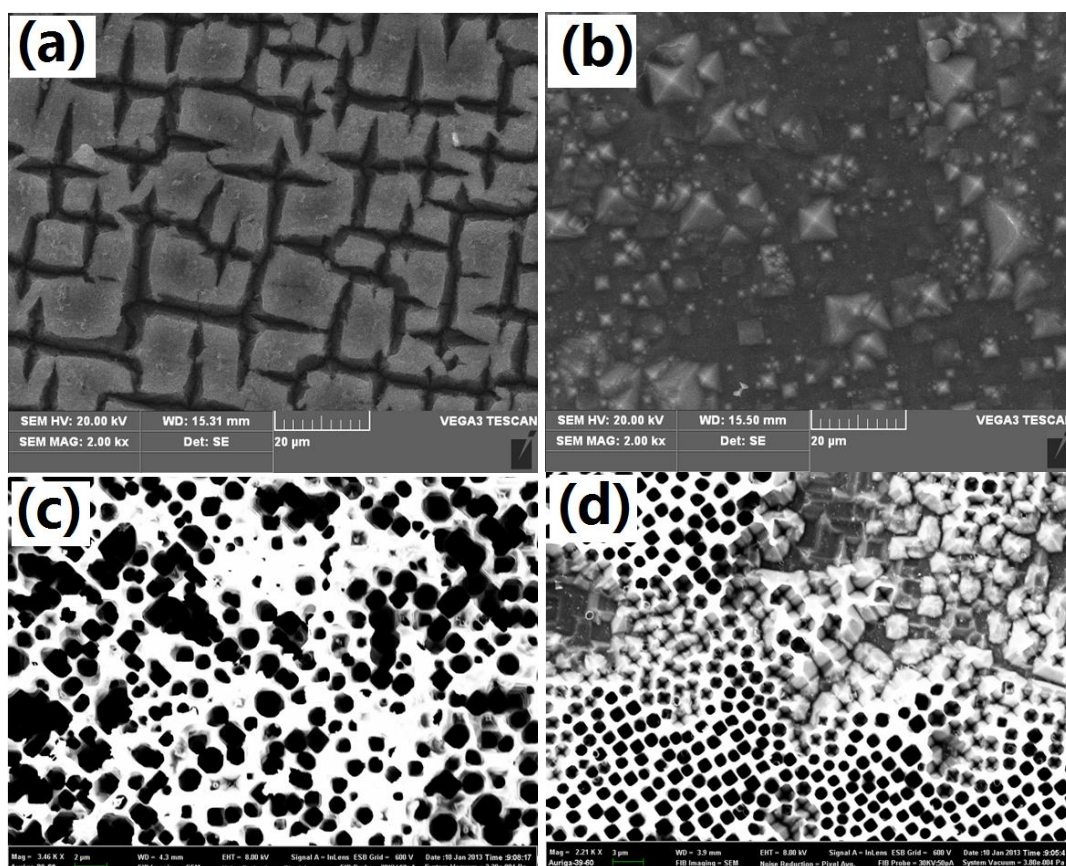


Figure 9. SEM images for f-PS corrosion in 1.0 M KOH for different time at 318 K, (a) before corrosion, (b) after f-PS layer removing, (c) corrosion for 10 min and (d) corrosion for 48 min.

Fig. 9 showed scanning electron microscope (SEM) images of f-PS corrosion in 1.0 M KOH for different time at 318 K. Before corrosion, the cracks could be seen on the surface of f-PS, and there

were no micropores (Fig. 9a). Along with the corrosion reaction, the porous structure (Fig. 9c-d) was clearly seen after the f-PS corrosion in 1.0 M KOH for different time (10 and 48 min). The f-PS sample immersed in 1.0 M KOH for 48 min was being discovered by bumpy silicon substrate, the pyramid-shaped silicon tip, imperfect micropores and perfect micropores. The image of silicon substrate with f-PS layer completely removed (58 min) is shown in Fig. 9b. At the same time, it was clear that the pyramid-shaped silicon tip was perpendicular to the surface of silicon substrate.

4. CONCLUSIONS

Porous silicon samples were fabricated by electrochemical anodization of silicon wafers in a solution of 1:1 (v/v) EtOH(99.5%)/HF(40%). After fabrication, the corrosion of f-PS in KOH solution in the absence and presence of ethanol was systemically studied by weight loss measurements, scanning electron microscope and electrochemical methods. Results showed that with increasing temperature and concentration of KOH solution the corrosion rate increased. The corrosion rate was accelerated greatly with additional ethanol in 1.0 M KOH. And it found that temperature and composition of KOH solution can affect the detection accuracy of weight loss measurements to measure the porosity of PS. In addition, the activation parameters (E_a , A , ΔH_a and ΔS_a) for f-PS corrosion in 1.0 M KOH were obtained.

Reference

1. A. Uhler, *Bell Syst. Tech. J.*, 35 (1956) 333.
2. D.R. Turner, *J. Electrochem. Soc.*, 105 (1958) 402.
3. L.T. Canham, *Appl. Phys. Lett.*, 57 (1990) 1046.
4. A.G. Cullis, L.T. Canham and P.D.J. Calcott, *J. Appl. Phys.*, 82 (1997) 909.
5. D. Chakravarty, B.V. Sarada, S.B. Chandrasekhar, K. Saravanan and T.N. Rao, *Mater. Sci. Eng. A*, 528 (2011) 7831.
6. W.A. Badawy, *J. Alloy. Compd.*, 464 (2008) 347.
7. C.K. Sheng, W.M.M. Yunus, W.M.Z.W. Yunus, Z.A. Talib and A. Kassim, *Physica B*, 403 (2008) 2634.
8. J.D. Benjamin, J.M. Keen, A.G. Cullis, B. Innes and N.G. Chew, *Appl. Phys. Lett.*, 49 (1986) 716.
9. H.Y. Zhang, Z.H. Jia, X.Y. Lv, J. Zhou, L.L. Chen, R.X. Liu and J. Ma, *Biosens. Bioelectron.*, 44 (2013) 89.
10. G. Toker, R. Sagi, S.B. Nachum and M. Asscher, *Chem. Phys.*, 138 (2013) 044710-1.
11. C.Y. Zhan, P.K. Chu, D. Ren, Y.C. Xin, K.F. Huo, Y. Zou and N.K. Huan, *Int. J. Hydrogen Energy*, 36 (2011) 4513.
12. W. Lang, P. Steiner, A. Richter, K. Marusczyk, G. Weimann and H. Sandmaier, *Sens. Actuators A: Phys.*, 43 (1994) 239.
13. I.I. Ivanov, V.A. Skryshevsky, T. Nychporuk, M. Lemiti, A.V. Makarov, N.I. Klyui and O.V. Tretyak, *Renew. Energ.*, 55 (2013) 79.
14. C. Mazzdeni and L. Pavesi, *Appl. Phys. Lett.*, 67 (1995) 2983.
15. B. Unal, A.N. Parbukov and S.C. Bayliss, *Opt. Mater.*, 17 (2001) 79.
16. F.A. Harraz, *Phys. Stat. Sol. C*, 8 (2011) 1883.
17. J. Kanungo, S. Maji, H. Saha and S. Basu, *Mater. Sci. Eng. B*, 167 (2010) 91.

18. K. Behzad, W.M.M. Yunus, Z.A. Talib, A. Zakaria and A. Bahrami, *Mater.*, 5 (2012) 157.
19. J. Peckham and G.T. Andrews, *Thin Solid Films*, 520 (2012) 2526.
20. K. Kordás, J. Remes, S. Beke, T. Hu and S. Leppävuori, *Appl. Surf. Sci.*, 178 (2001) 190.
21. M. Banerjee, E. Bontempi, S. Bhattacharya, S. Maji, S. Basu and H. Saha, *J. Mater. Sci.: Mater. Electron.*, 20 (2009) 305.
22. M.D. Li, M. Hu, W.J. Yan, S.Y. Ma, P. Zeng and X. Qin, *Electrochim. Acta*, 113 (2013) 354.
23. M.A. Hegazy, A.M. Badawi, S.S. A. E. Rehim and W.M. Kamel, *Corros. Sci.*, 69 (2013) 110.
24. Q. Deng, N.N. Ding, X.L. Wei, L. Cai, X.P. He, Y.T. Long, G.R. Chen and K.X. Chen, *Corros. Sci.*, 64 (2012) 64.
25. O. Bisi, S. Ossicini and L. Pavesi, *Surf. Sci. Rep.*, 38 (2000) 1.
26. E.J. Anglin, L.Y. Cheng, W.R. Freeman and M.J. Sailor, *Adv. Drug. Deliv. Rev.*, 60 (2008) 1266.
27. K.L. Jarvis, T.J. Barnes and C.A. Prestidge, *J. Colloid. Interface. Sci.*, 363 (2011) 327.
28. J. Riikonen, M. Salomaki, J.V. Wonderen, M. Kemell, W.J. Xu, O. Korhonen, M. Ritala, F.M. Millan, J. Salonen and V.P. Lehto, *Langmuir*, 28 (2012) 10573.
29. M.J. Sailor, *Porous Silicon in Practice*, Wiley-VCH: Gilman, 2012.
30. C.G. Kang, M.S. Kang, J.H. Yang, J.H. Jin, S.I. Hong and N.K. Min, *J. Korean Phys. Soc.*, 42 (2003) 693.
31. S. Setzu, S. Létant, P. Solsona, R. Romestain and J.C. Vial, *J. Lumin.*, 80 (1998) 129.
32. C. Lai, X.M Li, D.X. Zhang, Z. Xiang, W.J. Yang, X.G. Guo, *Mater. Chem. Phys.*, 144 (2014) 355.
33. C. Lai, X.M Li, C.L Liu, X.G. Guo, Z. Xiang, B.Xie, L.K.Zou, *Mater. Sci. Semicon. Proc.*, 26 (2014) 501.
34. E.E. Ebenso, *Nigerian J. Chem. Res.*, 6 (2001) 8.
35. I.B. Obot and N.O. Obi-Egbedi, *Corros. Sci.*, 52 (2010) 198.
36. M. Balaguer and E. Matveeva, *J. Nanopart. Res.*, 12 (2010) 2907.
37. P.B. Mathur and T. Vasudevan, *Corros.*, 38 (1982) 171.
38. I. Ahamad, R. Prasad and M.A. Quraishi, *Corros. Sci.*, 52 (2010) 933.
39. N. Soltani, M. Behpour, S. M. Ghoreishi and H. Naeimi, *Corros. Sci.*, 52 (2010) 1351.
40. I. Ahamad, R. Prasad and M.A. Quraishi, *Corros. Sci.*, 52 (2010) 1472.

© 2015 The Authors. Published by ESG (www.electrochemsci.org). This article is an open access article distributed under the terms and conditions of the Creative Commons Attribution license (<http://creativecommons.org/licenses/by/4.0/>).